ASM Handbook, Volume 11, *Failure Analysis and Prevention*
B. Miller, R. Shipley, R. Parrington, D. Dennies, editors
DOI 10.31399/asm.hb.v11.a0006780

Creep and Stress-Rupture Failures

Richard P. Baron, Engineering Systems, Inc.

HIGH TEMPERATURE AND STRESS are common operating conditions for various parts and equipment in many industries. The principal types of elevated-temperature mechanical failure are creep and stress rupture, stress relaxation, low- and high-cycle fatigue, thermal fatigue, tension overload, and combinations of these, as modified by environment. Generally, the type of failure is established by examination of fracture surfaces and comparison of component operating conditions with available data on creep, stress-rupture, tension, elevated-temperature fatigue, and thermal fatigue properties. Such an analysis is usually sufficient for most failure investigations, but a more thorough analysis can be required when stress, time, temperature, and environment have changed the metallurgical structure of the component (see, for example, the section "Metallurgical Instabilities" in this article).

This article briefly reviews the applied aspects of creep-related failures, where mechanical strength of a material becomes limited by creep rather than by its elastic limit. The majority of information provided is applicable to metallic materials, and only general information regarding creep-related failures of polymeric materials is given. Detailed information regarding the creep and creep-rupture characteristics of polymeric materials is provided in *Engineering Plastics*, Volume 2 of *Engineered Materials Handbook*, 1988.

Creep deformation produces sufficiently large changes in the dimensions of a component to either render it useless for further service or cause fracture. When excessive creep deformation causes the material to reach or exceed some design limit on strain, the term *creep failure* is used. For example, a creep failure of a cobalt-base alloy turbine vane is shown in Fig. 1. The bowing is the result of a reduction in creep strength at the higher temperatures from overheating.

Creep deformation can also result in the complete separation or fracture of a material and the breach of a boundary or structural support. Fracture can occur from either localized creep damage or more widespread bulk damage caused by the accumulation of creep strains over time. Structural components that are vulnerable to bulk creep damage typically are subjected to uniform loading and uniform temperature distribution during service. The life of such a component is related to the creep-rupture properties, and the type of failure is referred to as stress rupture or creep rupture. Stress or creep rupture is likely to occur when damage is widespread with uniform stress and temperature exposure, as in the situation of thin-section components (such as steam pipes and boiler tubes).

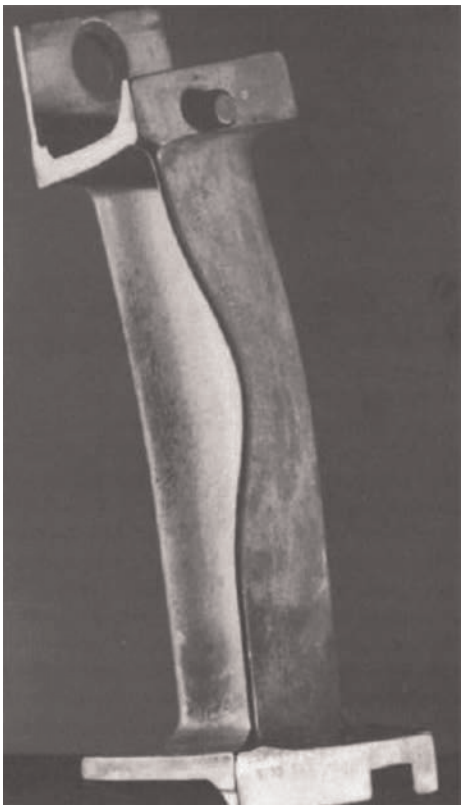

Fig. 1 Creep damage (bowing) of a cobalt-base alloy turbine vane from overheating

Creep damage can also be localized, particularly for thick-section components that are subjected to gradients in stress (strain) and temperature. An example of a creep-related crack is shown in Fig. 2. Cracks can develop at a critical location and propagate to failure before the end of the predicted creep-rupture life. Creep cracking can also originate at a stress concentration or at preexisting defects in the component. In these cases, most of the life of the component is spent in crack growth. This involves assessment of fracture resistance rather than a strength assessment based on bulk creep rates and time to stress rupture. Therefore, creep life assessment can involve evaluation of both creep strength (i.e., creep rate, stress rupture) and resistance to fracture under creep conditions.

Failures from creep deformation depend on material, time-temperature exposure, loading conditions, component geometry, and environmental and material structural factors. Also, it is not unusual to find other contributing factors, such as corrosion, fatigue, and material defects, involved in creep and stress-rupture failures. This article briefly reviews these

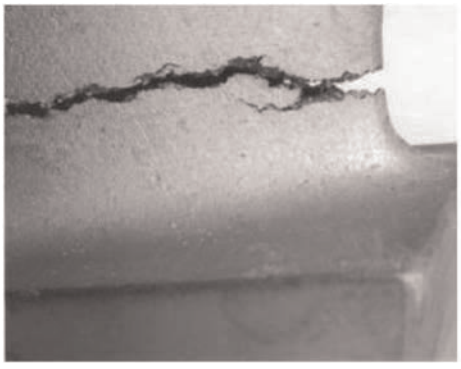

Fig. 2 Creep crack in a turbine vane. Courtesy of M. Chaudhari, Columbus Metallurgical Services

factors as they relate to creep behavior and associated failures of materials used in high-temperature applications. The complex effects of creep-fatigue interaction are also discussed, although more detail on this is described in the article "Thermomechanical Fatigue: Mechanisms and Practical Life Analysis" in this Volume. Life assessment is also covered in the article "Elevated-Temperature Life Assessment for Turbine Components, Piping, and Tubing" in *Failure Analysis and Prevention*, Volume 11 of the *ASM Handbook*, 2002.

Brief History

The study of creep can be traced back to 1904 when Trouton and Rankine (Ref 1) determined a logarithmic dependence between "stretch" and time for lead. In 1905, Phillips (Ref 2) detailed the creep experiments of copper, platinum, silver, gold, and steel wires and opined that a logarithmic dependence between stretch and time existed for copper, platinum, silver, and gold wires, but the behavior of steel wires did not follow the same relationship. These initial experiments by Trouton and Phillips were performed at room temperature. In 1910, Andrade (Ref 3) furthered the study of creep and even studied the effect of temperature, performing a series of tests at 162 °C (323 °F). Andrade's experiments also revealed the importance of running creep tests under a constant stress instead of a constant load. Each of these early studies on creep revealed a change in the creep response of a material as a function of time.

Bulk Creep Behavior

Some key material properties at high temperature are thermal expansion coefficient, stress rupture, elastic modulus, fatigue life, and oxidation resistance. Total strain at temperature is given by the sum of elastic stress-strain modulus, thermal expansion strain, and creep strain. Change in elastic modulus with temperature cannot be neglected at higher homologous temperatures. Parametric modeling of creep and stress-rupture behavior often normalizes the stress with the modulus.

One way to avoid creep failure is to select the proper material based on parametric extrapolation of creep properties. In general, creep occurs in any material at a temperature where atoms become sufficiently mobile to allow time-dependent rearrangement of structure. Creep behavior of a polycrystalline metal or alloy often is considered to begin at approximately one-third to one-half of its melting point (~0.3 to 0.5 T_M) measured on an absolute temperature scale (degrees Kelvin or Rankine). However, this rule of thumb is not necessarily the criteria for engineering design. Creep deformation becomes important when mechanical strength of a metal becomes limited by creep rather than by yield strength. This transition in engineering design is not directly related to melting temperature; consequently, the temperature at which the mechanical strength of a metal becomes limited by creep, rather than by elastic limit, must be determined individually for each metal or alloy.

Approximate temperatures at which creep behavior begins for several metals and alloys are listed in Table 1. Low-melting-point metals (such as lead, tin, and high-purity aluminum) can deform by creep at or a little above room temperature. In contrast, refractory body-centered cubic metals (such as tungsten and molybdenum) and nickel-base superalloys require temperatures near 1000 °C (1830 °F) to activate the onset of creep deformation engineering significance. Typical materials and application temperatures of some creep-resistant alloys are listed in Table 2.

The creep behavior of polymeric materials is more complex, because most plastics respond as true solids over a limited time frame, but over time and under load, they can behave as extremely viscous liquids (Ref 4). The response of a polymeric material to temperature under load is dependent on its glass transition temperature (T_g), which is defined as the transition temperature between the glassy, or brittle, and relatively flexible phases of a polymer. This temperature, in turn, depends on the average molecular weight of a thermoplastic polymer or the degree of cross-linking for a thermoset polymer. Polymers used above their T_g can readily creep under an applied load, whereas those polymers, like most engineering plastics, used below their T_g are more resistant to creep failure (Ref 5).

Constant-load bulk deformation creep curves typically (but not always) consist of three distinct stages (Fig. 3a). The first stage (called primary creep) is the region of the initial instantaneous elastic strain from the applied load, followed by a region of increasing plastic strain at a decreasing strain rate (Fig. 3b). Following the first stage of primary creep is the region of secondary creep, where the creep rate is nominally constant at a minimum rate, generally known as the minimum creep rate. The stage of secondary creep is sometimes referred to as the region of steady-state creep, because the creep rate is often nominally constant for some duration. Finally, there is a region of drastically increased strain rate with rapid extension to fracture in the third stage of tertiary creep. Constant-stress tests (as opposed to constant-load tests) often do not show tertiary behavior (Fig. 4).

Creep and stress-rupture data usually are obtained under constant-load test condition, and therefore, the stress in the gage section varies with time. However, it is sometimes desirable or necessary to obtain test data under constant-stress conditions, where the applied load is adjusted as the length of the specimen changes to maintain constant stress on the specimen. Constant-stress testing is used to accurately determine differences between the temperature dependence and the stress dependence of creep behavior. In general, the form of creep strain (in the form of primary, secondary, and tertiary stages) under constant-stress conditions is the same as those for constant load. However, the duration spent in primary and secondary creep under constant stress can be much longer than under an identical engineering stress (constant load). Therefore, rupture life is longer under constant-stress conditions.

It is also important to note that the region of initial elastic strain under load (ε_0 in Fig. 3a) is not identified as a stage of creep deformation, because it is common practice to ignore this contribution to total strain when plotting creep curves. Consequently, creep curves generally show only the time-dependent plastic strain that follows the initial elastic (and possibly plastic) strain. Although this procedure is acceptable for research and investigation, the initial strain, which can amount to a substantial fraction of the total strain, should not be

Table 1 Approximate temperatures for onset of creep behavior for select alloy groups

Alloy group	Temperature for onset of creep		
	°C	°F	T as ratio of T_M, K
Aluminum alloys	150–200	300–390	0.48–0.54 T_M
Titanium alloys	315	600	0.3 T_M
Low-alloy steels	370	700	0.36 T_M
Austenitic, iron-base heat-resisting alloys	540	1000	0.49 T_M
Nickel- and cobalt-base heat-resisting alloys	650	1200	0.56 T_M
Refractory metals and alloys	980–1540	1800–2800	0.4–0.45 T_M

Table 2 Typical elevated temperatures in engineering applications

Application	Typical materials	Typical temperatures, K	Homologous temperatures, T/T_M
Rotors and piping for steam turbines	Cr-Mo-V steels	825–975	0.45–0.50
Pressure vessels and piping in nuclear reactors	316 stainless steel	650–750	0.35–0.40
Reactor skirts in nuclear reactors	316 stainless steel	850–950	0.45–0.55
Gas turbine blades	Nickel-base superalloys	775–925	0.45–0.60
Burner cans for gas turbine engines	Oxide-dispersion-strengthened nickel-base alloys	1350–1400	0.55–0.65

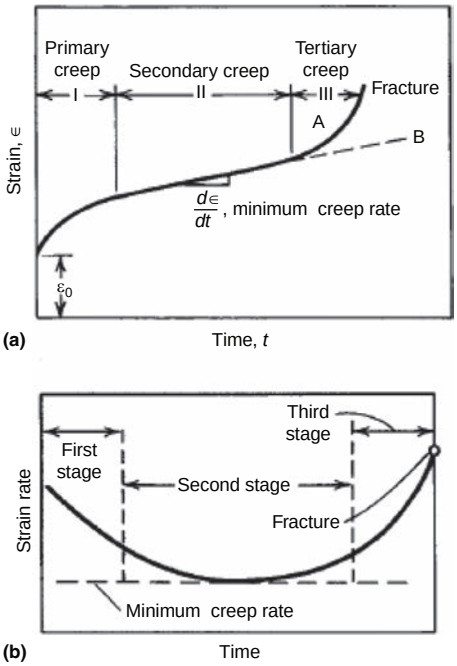

Fig. 3 Stages of creep deformation. (a) Strain curve for the three stages of creep under constant-load testing (curve A) and constant-stress testing (curve B). (b) Relationship of strain rate, or creep rate, and time during a constant-load creep test. The minimum creep rate is attained during second-stage creep.

omitted from design studies and failure analyses. Therefore, as stated previously, modulus at temperature is of importance. Thermal expansion can impose additional strain and must also be considered.

The classical pattern of creep deformation fits many materials under various test conditions. However, even though it is relatively easy to quantify damage in laboratory creep tests conducted at constant temperature and load (or stress), components in service hardly ever operate under constant conditions. Start-stop cycles, reduced power operation, thermal gradients, and other factors result in variations in stresses and temperatures. Therefore, damage rule procedures are used to estimate cumulative damage under changing exposure conditions. In addition, creep behavior can depart from classical creep curves even under controlled laboratory testing. The following sections briefly review the microstructural changes and bulk mechanical behavior of classical creep behavior and some instances of nonclassical behavior. This is followed by a brief description of microstructural changes and damage from creep deformation.

Classical Creep Behavior

During creep, significant microstructural changes occur on all levels. For metals on the atomic scale, dislocations are created and forced to move through the material. This

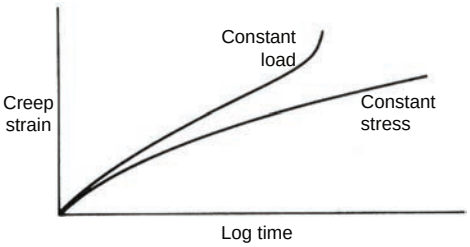

Fig. 4 Creep curves produced under constant-load and constant-stress conditions. Reprinted with permission from Wiley. Source: Ref 6

leads to work hardening as the dislocation density increases and the dislocations encounter barriers to their motion. An ever-diminishing creep rate results at low temperatures. However, if the temperature is sufficiently high, dislocations rearrange and annihilate through recovery events. For polymeric materials at the atomic scale, creep causes a reorganization of molecules to minimize localized stresses (Ref 5). During creep deformation, the material also is progressively degraded or damaged as the amount of creep strain increases over time.

Primary Creep

Primary creep, also known as transient creep, represents a stage of adjustment during which rapid, thermally-activated plastic strain occurs. In metals, the combined action of hardening and recovery processes during primary creep can lead to the formation of a stable distribution of subgrains or loose, three-dimensional dislocation networks in some materials, or an approximately uniform dislocation distribution without subgrains in other materials. These stable dislocation configurations are maintained and are characteristic of second-stage creep. Primary creep occurs in the first few moments after initial strain and decreases in rate as crystallographic imperfections within the metal undergo realignment. Similarly, in polymers, the primary creep stage is characterized by a reorganization of molecules. This realignment of crystallographic imperfections in metals or molecules in polymers leads to secondary creep.

Because a variety of structural processes can be involved, and because the rates and direction of these processes can vary with time and temperature, departures from classical creep curves could be overlooked, unless accurate creep readings are taken at sufficiently close intervals, particularly during early stages of creep.

Secondary Creep

Secondary creep is an equilibrium condition between the mechanisms of work hardening and recovery; it is also known as steady-state creep. As previously noted, secondary creep is essentially a transition between primary and tertiary creep, where the creep rate reaches a minimum value (Fig. 3b). This often occupies the major portion of the duration of the creep test, and the strain rate in this region for many creep-resistant materials is sufficiently constant to be considered as a steady-state creep rate. For these materials, the minimum creep rate is a steady-state value that can be empirically related to rupture life and is widely used in research and engineering studies.

However, the concept of a steady creep rate during secondary creep is more of an empirical concept than a mechanistic description of material behavior. Nonuniform deformation and changes in stress and structural conditions at high temperature are factors that can influence the creep rate. Thus, the process of secondary creep can be more complicated than a constant, steady-state mechanistic condition. Nonetheless, the observation of steady creep rates over a large portion of creep-test curves is an important empirical result with practical value. The concept of a steady-state creep rate should only be viewed as an experimental result, not as an underlying material condition. Variations from structural instabilities, environmental exposure, and changing stress-temperature conditions are additional factors as well.

Tertiary Creep

Tertiary creep refers to the region of increasing rate of extension, which is followed by fracture. Primary creep has no distinct endpoint, and tertiary creep has no distinct beginning. Principally, it can result from structural changes, such as recrystallization or reorganization under load, which promote rapid increases in deformation. For metals, recrystallization is accompanied by work hardening, which is insufficient to retard the increased flow of metal and can correspond to the onset of necking in some alloys.

In service and in creep testing, tertiary creep can be accelerated by a reduction in cross-sectional area resulting from cracking, necking, and viscous flow. Environmental effects, such as oxidation in metals, that reduce cross section can also initiate tertiary creep and increase the tertiary creep rate. In many commercial creep-resistant metallic alloys, tertiary creep is apparently caused by inherent deformation processes and occurs at creep strains of 0.5% or less. In designing components for service at elevated temperatures, data pertaining to the elapsed time and extension that precede tertiary creep are of the utmost importance; design for creep resistance is based on such data. However, the duration of tertiary creep is also important, because it constitutes a safety factor that can enable detection of a failing component before catastrophic fracture.

Nonclassical Creep Behavior

Although the classical pattern of creep deformation can be made to fit many materials

and test conditions, the relative duration of the three stages differs widely with materials and conditions. For instance, in many superalloys and other materials in which a strengthening precipitate continues to age at creep temperatures, brief primary creep often transitions to a long, upward increase of creep rate, with only a point of inflection identifying the secondary creep regime.

For example, aging of normalized and tempered 0.5Cr-0.5Mo-0.25V alloy steel during creep under 80 MPa (11.6 ksi) stress at 565 °C (1050 °F) has been reported to cause the creep curve to effectively exhibit only a continuously increasing creep rate to fracture (Ref 7). For twice the amount of stress, the creep curve in this case followed the classical trends. In other alloys, such as titanium alloys, with limited elongation before fracture, the tertiary stage can be brief and could show little increase in creep rate before rupture occurs. A more obvious departure from classical behavior develops during the early portion of many tests, when precise creep measurements are taken. When 34 ferritic steels were studied for as long as 100,000 h at temperatures ranging from 450 to 600 °C (840 to 1110 °F), step-form irregularities were observed, with an extended period of secondary creep preceded by a lower creep rate of shorter duration during primary creep (Ref 8).

Under certain conditions, some metals also may not exhibit all three stages of plastic extension. For example, at high stresses or temperatures, the absence of primary creep is not uncommon, with secondary creep or, in extreme cases, tertiary creep following immediately upon loading. At the other extreme, notably in cast alloys, no tertiary creep stage can be observed, and fracture can occur with only minimum extension.

Oxide and Nitride Strengthening

An entirely different source of variation from classical creep can occur from environmental reactions at high temperature. For example, tests longer than 50 h with 80Ni-20Cr alloys at 815 and 980 °C (1500 and 1800 °F) showed a deceleration of creep after the normal tertiary stage was reached, resulting in a second period of steady-state creep and later, another period of last-stage creep (Ref 9). This behavior is due to oxide strengthening, which prolonged rupture life and caused a slope decrease in curves of log stress versus log rupture life. Oxides and nitrides formed on the surfaces of the intercrystalline cracks that occur extensively during tertiary creep. Observed interconnection of the bulk of these cracks added substantially to strengthening against creep deformation in the late stages of the tests. This effect also has been observed in 99.8% Ni tested at 815 °C under 20.7 MPa (3000 psi) stress (Ref 10).

Microstructural Changes during Classical Creep

Metallic Materials

During creep, significant microstructural changes occur on all levels. As mentioned previously, on the atomic scale, dislocations are created and forced to move through the material, which leads to work hardening as dislocation density increases and dislocations encounter barriers to their motion. At low temperatures, an ever-diminishing creep rate results, but if the temperature is high enough, dislocations rearrange and annihilate through recovery events.

On a more macroscopic scale, creep deformation also produces microstructural changes, such as slip bands, grain-boundary sliding, cavity formation and growth, and cracking (grain boundary, interphase boundary, and transgranular). Other potential microstructural changes include in situ graphitization that occurs in iron-base alloys without adequate carbide-stabilizing elements present. Iron carbide (cementite) decomposes to graphite and iron. Chromium is typically added to prevent this. In situ graphitization is also affected strongly by molybdenum content and deoxidation practice. The extent of these microstructural changes is generally increased near fracture sites, compared with other regions.

The microstructure of a creep or stress-rupture specimen after elevated-temperature exposure rarely resembles the initial microstructure prior to exposure. Of course, most materials are not thermodynamically stable; thus, prolonged exposure under creep conditions can result in microstructural changes, such as the precipitation of new phases, dissolution or growth of desired phases, grain growth, and so on. Many of the structural changes can be duplicated through simple heat treatment. However, some microstructural changes only occur under the combined influence of stress and temperature. For example, under normal isothermal annealing, the cube-shaped γ-(Ni_3Al) strengthening phase in nickel-base superalloy NASAIR 100 undergoes Ostwald ripening, characterized by an increase in particle size without any shape change. However, during creep testing, the individual precipitates grow together rapidly and form thin γ plates, where the long dimensions of each plate are perpendicular to the stress in tensile creep and parallel to the applied stress in compressive creep (Ref 11).

The changes in microstructure that occur during creep testing can affect properties. Although such changes may be unavoidable, in many cases, thermomechanical processing schedules can be established to influence the changes so that they tend to strengthen the material or minimize the overall effect. For example, if a heterogeneous precipitate is formed during creep, a simple heat treatment or cold work followed by annealing prior to testing should yield a homogeneous distribution of precipitates.

Microstructural changes due to the combined influence of temperature and stress can be difficult to evaluate. Therefore, simulation of creep exposure prior to actual use is sometimes necessary, where tested and untested materials are examined and compared. Complete microstructural examination should be an essential part of any creep experiment and failure investigation. At a minimum, microstructure and phase identification should be compared for specimens near and farther away from the fracture site. Comparison of these can help identify relevant deformation mechanisms, environmental effects, and microstructural changes. Such information is vital for interpreting and understanding creep behavior.

Generally, creep (distortion) failures are recognized by local ductility and multiplicity of intergranular cracks (Fig. 5). However, creep deformation of engineering significance can also occur before intergranular fracture initiates. Stress-rupture data (log stress versus log time to failure) typically show an inflection when a change in fracture mechanism occurs, including significant formation of sigma phase and a change in fracture from transgranular to intergranular. Measurements of fracture strain also show a minimum when the mechanism changes.

Void Formation

The most common form of microstructural change is the accumulation of nucleation and growth of voids. Void growth is well understood, because voids grow by the same mechanisms that cause creep deformation. In contrast, void nucleation is not fully understood, although it appears to be the result of strain "misaccommodation," similar to crack nucleation in some low-temperature fractures (Ref 12). For the high-temperature case, two adjacent grains can move at different creep rates. If the rates cannot be made to match, a gap forms between the grains. In general, higher creep rates cause voids to form earlier during the creep process. Thus, any material alteration that leads to a lower creep rate also improves creep strength.

Creep damage begins as small holes or cavities that typically form at grain boundaries or second phases. With time and stress, the holes or cavities can link up and form cracks, by both void growth (diffusion controlled) and by shear strain on the grain boundary, which eventually lead to failure of the component. The damage is progressive and can occur in bulk or, more predominantly, in localized regions. The formation of creep cracks is usually very localized in thick-section components; they form in welds, bends, and other highly stressed regions.

Polymeric Materials

Unlike metallic materials, polymeric materials do not exhibit a distinct crystalline

structure but instead are either amorphous or semicrystalline. The degree of crystallinity determines the mechanical properties of the component. For amorphous polymers, properties are dependent on chain flexibility and cross linking. Nevertheless, creep damage in polymers is realized through the formation of microscopic cracking and crazing and, potentially on a macroscopic scale, whitening.

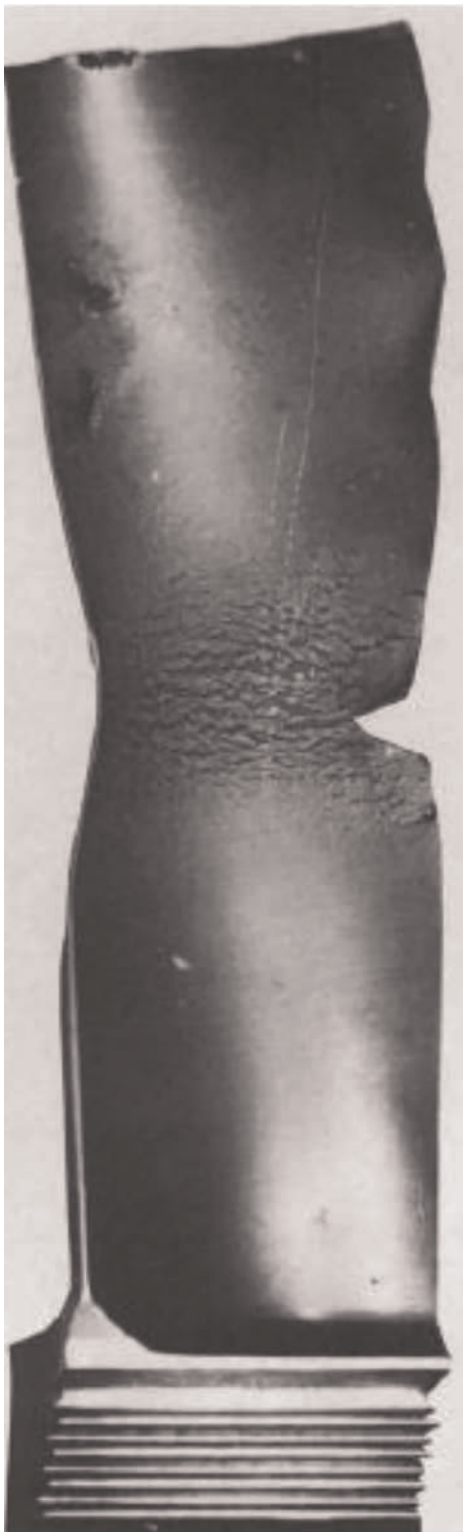

Fig. 5 Typical creep deformation and intergranular cracking in a jet-engine turbine blade. Courtesy of J. Schijve

Nondestructive Creep Damage Assessment of Metallic Materials

Determining the extent of progressive damage is an important imperative for regular inspections of components exposed to elevated temperatures. The most direct method of creep assessment involves metallographic examination of sections cut from components. For components still in operation, this method necessarily renders the component unfit for service. Thus, methods of assessing the condition of a component through nondestructive testing (NDT) are of great value. Sposito et al. (Ref 13) provide a comprehensive review of available NDT techniques, including their advantages and disadvantages. The following provides a brief description of some of the techniques.

Replication Methods

Surface replication, which enables examination of microstructural damage without cutting sections from the component, is a well-known sample-preparation technique that can be used to assess the condition of high-temperature power plant and petrochemical components from creep damage. Plastic replicas lend themselves to in-plant nondestructive examination because of their relative simplicity and short preparation time. Plastic replicas can be examined using light optical microscopy, scanning electron microscopy, and transmission electron microscopy, depending on the resolution required.

Replication techniques are sufficiently sophisticated to enable classifying microstructural damage (Fig. 6), which can be directly correlated to life fractions. Bulk damage from creep deformation typically occurs by the nucleation and growth of voids either within grains or, more commonly, along grain boundaries. Internal voids initially nucleate during creep deformation and then grow. A distinct correlation exists for these data, such that a minimum and maximum remaining life fraction can be specified (Table 3). The presence of detrimental microstructural features, including sigma phase and graphitization, can also be monitored.

Hardness Measurements

Creep damage of metallic materials in the power-generation industry can be monitored through in situ Vickers hardness tests. For example, in chromium-molybdenum steels, an almost linear decrease in hardness has been observed during the secondary creep stage, suggesting a good correlation between Vickers hardness and creep life. However, Vickers hardness tests are susceptible to variability and scatter depending on surface condition, with decarburized surfaces yielding erroneously lower hardness values, and local microstructural variations, such as at weld locations. Thus, using hardness measurements as a means to assess creep life should only be restricted when extensive data for a specific heat of material are available.

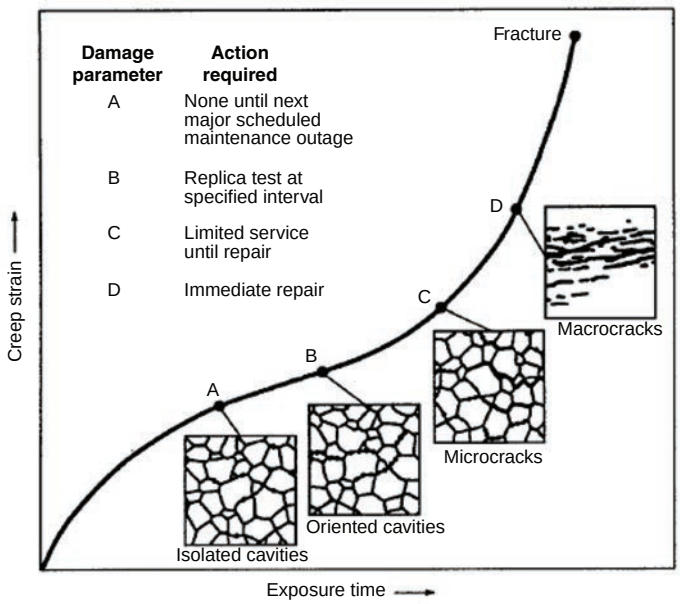

Fig. 6 Creep life assessment based on cavity classification in boiler steels. Source: Ref 14

Bulk Volume Creep Assessment

The aforementioned techniques are restricted to evaluation of the surface condition of components. However, recently, conventional NDT techniques, such as ultrasonic and eddy-current testing, and nonconventional NDT techniques, including potential drop and positron annihilation, have been used to assess the volumetric creep condition of a component. The results provided by these techniques are still not completely understood, limiting their implementation.

The qualitative-quantitative relation is advantageous, because data from NDT can be predictive in terms of generating a conservative minimum- and maximum-life estimate. The maximum life is useful in a predictive maintenance environment, because it would dictate the planning of future repairs or replacement. Various damage rules are also used to approximate remaining time to rupture for components that have undergone prolonged high-temperature exposure. Damage rules and postservice creep testing are discussed further in the article "Assessment and Use of Creep-Rupture Properties" in *Mechanical Testing and Evaluation*, Volume 8 of the *ASM Handbook*, 2000 (Ref 16). Component creep life determination methods from collected data are available in standard fitness-for-service publications (Ref 17).

Stress Rupture

In the design of components for service at elevated temperature, both strength and stress-rupture ductility must be considered. Typically, for metallic materials, these properties are determined quantitatively by smooth-bar stress-rupture tests. In most service applications, components are subjected to complex stresses, including stress concentrations arising from inherent flaws in the material and those stemming from design, limiting the applicability of smooth-bar laboratory testing. Fortunately, service conditions can be partly reproduced in the laboratory by use of the notched-bar test. Notched-bar stress-rupture tests are of principal interest for metallic materials due to the relationship between stress-rupture ductility and the ratio of notched-bar to smooth-bar stress-rupture strength.

Thus, prevention of creep-induced fracture involves the consideration of both material strength and damage tolerance, much as in static design. The chromium-molybdenum steels, stainless steels, and Cr-Mo-V steels, which are commonly used in high-temperature service, are considered to be creep-ductile materials with the ability to sustain significant amounts of crack growth before failure. However, most engineering alloys can lose ductility during high-temperature service, because the diffusion of impurities to the grain boundaries becomes more pronounced. Formation of precipitates can also beneficially influence creep behavior, as discussed in the section "Metallurgical Instabilities" in this article.

Table 3 Correlation of damage level and life fraction consumed

Damage level	Consumed life fraction range X	Remaining life factor$(1/X - 1)$	
		Minimum	Maximum
1	0.00–0.12	7.33	Unknown
2	0.04–0.46	1.17	24.00
3	0.3–0.5	1.0	2.33
4	0.3–0.84	0.19	2.33
5	0.72–1.00	0 = failed	0.39

Source: Ref 15

Stress-Rupture Strength

The stress-rupture strength of a metallic material is determined by measuring the time to fracture as a function of temperature and applied stress. Logarithmic (log-log) plots of normal stress (σ) versus rupture life (RL) provide an indication of metallurgical instabilities. These instabilities are delineated by the occurrence of new straight-line segments of changed slope on the log-log plot, as shown by inflection points *A*, *B*, *N*, *O*, and *Y* in Fig. 7 for a well-known nickel-base heat-resisting alloy. Stress rupture is a variable-rate process; straight lines on log σ-log RL plots are simply approximations of a continuously varying curve.

Several parameters have been used for comparison and interpolation of stress-rupture data for metallic materials. A widely used parameter is the Larson-Miller parameter (LMP), defined by F.R. Larson and J. Miller, who correctly surmised creep to be thermally activated. This relationship enables describing the creep rate by an Arrhenius-type expression (Ref 6). With a few assumptions, a material exhibits a constant LMP for a given applied stress. Thus, the LMP is useful to determine the remaining rupture life at a given applied stress, and it is defined by the following equation:

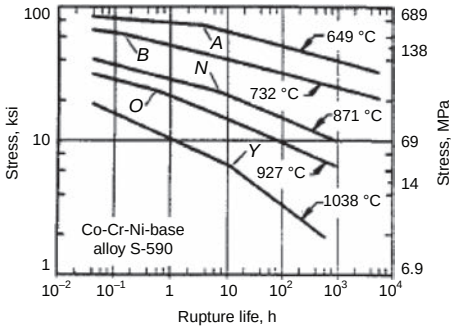

Fig. 7 Logarithmic plot of stress-rupture stress versus rupture life for Co-Cr-Ni-base alloy S-590. The significance of inflection points *A, B, N, O,* and *Y* is explained in the text. Source: Ref 18

$$\text{LMP} = T[C + \log t] \times 10^{-3}$$

where T is the test temperature in Rankine (°F + 460), t is the operating time in hours, and C is a material constant, approximately 20 for a low-alloy steel. Other parametric methods are discussed in the article "Elevated-Temperature Life Assessment for Turbine Components, Piping, and Tubing" in *Failure Analysis and Prevention*, Volume 11 of the *ASM Handbook*, 2002, and in the article "Assessment and Use of Creep-Rupture Properties" in Ref 16.

Stress-Rupture Ductility

While creep strength and rupture strength are given considerable attention as design and failure parameters, rupture ductility is an important mechanical property when stress concentrations and localized defects, such as notches, are a factor in design. Rupture ductility, which varies inversely with creep and rupture strength, influences the growth of cracks and defects and can be compared in terms of notch sensitivity.

In select service conditions, the amount of deformation is not critical, and relatively high rupture ductility can be used in design. Under such conditions, with the combined uncertainties of actual stress, temperature, and strength, it could be important that failure not occur without warning and that the metallic component retain high elongation and reduction in area throughout its service life. For instance, in the oil and chemical industries, many applications of tubing under high pressure require high long-time ductility, so that impending rupture is evident from the bulging of the tubes.

The two common measures of ductility are elongation and reduction of area. However, in tension-creep curves, there are two meaningful measures of elongation: true elongation, which is defined as the elongation at the end of the second stage of creep, and total elongation, which is the elongation at fracture. In some instances, elongation at fracture is mainly extension caused by crack separation. In others, it is mainly necking extension or extension resulting from other tertiary creep processes. However, uniform elongation nominally consists of extension resulting from nonlocalized creep processes only, although it frequently includes some elongation due to intergranular void formation. Generally, true elongation provides the more accurate representation of ductility in metals at elevated temperatures.

Ductility data from stress-rupture tests are generally erratic, especially for metal castings, even in replicate tests with data scatter at the same temperatures and stress, and variation in the measured strain at fracture varies with both stress and temperature. In some metals and alloys, the values of total elongation follow a smooth curve that either increases or decreases with increasing rupture time and temperature.

Ductility data typically show a minimum, initially increasing above room-temperature ductility, then going through a minimum, then increasing again, and finally dropping very fast near the melting point. The increase above the minimum in the curve is often assumed to be due to dynamic recrystallization.

Data on total elongation and reduction of area at various stress levels for a low-alloy steel at 540 °C (1000 °F) and a stainless steel at 705 °C (1300 °F) are provided in Table 4. Despite some difficulties in the interpretation of ductility data, common practice is to plot elongation versus rupture life, as in Fig. 8, which presents values for both total and true elongation at two different testing temperatures for the nickel-base alloy S-590. At both temperatures, an appreciable scatter of data points exists for total elongation (open circles in Fig. 8). The large differences between total and true elongation shown in Fig. 8 are a function of crack volume and distribution in tertiary creep. The differences in crack initiation and growth during the initial stages of creep can make only relatively small differences in total elongation. Thus, replicate tests can exhibit large differences in total elongation but very small differences in true elongation.

Table 4 Typical elevated-temperature ductility of a 1.25Cr-0.5Mo low-alloy steel and type 316 stainless steel

Time to rupture, h	Total elongation in 40 mm (1.5 in.), %	Reduction in area, %
1.25Cr-0.5Mo low-alloy steel at 540 °C (1000 °F)		
8.7	19.6	41
47.0	12.1	29
259.4	14.0	20
660.6	10.5	13
2162.0	17.6	32
Type 316 stainless steel at 705 °C (1300 °F)		
3.1	26.6	26
3.7	24.4	27
37.5	17.8	28
522.6	56.2	41
881.6	39.4	33

Stress-rupture ductility is an important factor in alloy selection. For example, in conventionally cast nickel-base heat-resisting alloys, a stress-rupture ductility of approximately 1% is common at 760 °C (1400 °F) compared with values above 5% for the strongest wrought heat-resisting alloys. Because component designs are frequently based on 1% creep, a low stress-rupture ductility could preclude the use of an alloy to its full strength potential. As shown by the schematic creep curves in Fig. 9, a higher rupture ductility for the same load and temperature conditions means a higher safety margin. Failure to compensate for an absence of ductility during tertiary creep can cause premature failures.

Creep Crack Growth

Components having localized damage, which is a result of nonuniform stress and temperature distribution found commonly in large structures, are more prone to fail as a result of creep crack propagation rather than stress rupture. Despite the sophisticated NDT methods of flaw detection that are available, defects and impurities are commonly present in all large components and can potentially escape detection. In the high-temperature regime, components can fail by the accumulation of time-dependent creep strains at these defects, which with time can evolve into cracks and eventually cause failure.

Most engineering metal alloys are highly plastic at elevated temperatures, and any preexisting crack can quickly become blunted. Under such conditions, creep is generally considered a net-section effect. In this case, the process of subcritical creep crack growth would not be characterized by the fracture-mechanics stress-intensity (K) parameter. Other methods are used to characterize creep crack growth in ductile metal materials used at high temperature, as described in more detail in the article "Elevated-Temperature Life Assessment for Turbine Components, Piping, and Tubing" in *Failure Analysis and Prevention*, Volume 11 of the *ASM* Handbook, 2002.

However, some high-temperature materials (such as intermetallics and some precipitation-hardening superalloys) are less ductile and can have creep crack growth that depends on the crack tip stress field. In these cases, the creep crack growth rate (da/dt) follows the conventional fatigue crack growth rate and can be correlated with K, the stress-intensity factor, with a power-law dependence as:

$$da/dt = \alpha K^n$$

where α and n are the curve-fitting parameters. The value of n varies between 1 and 8, depending on the stress dependence of the specific creep mechanism (Ref 19). A distinct threshold stress intensity is usually not observed, as shown in the general example in Fig. 10.

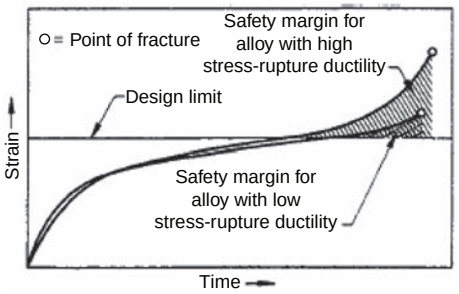

Fig. 9 Schematic creep curves for alloys having low and high stress-rupture ductility, showing the increased safety margin provided by the alloy with high stress-rupture ductility. Source: Ref 18

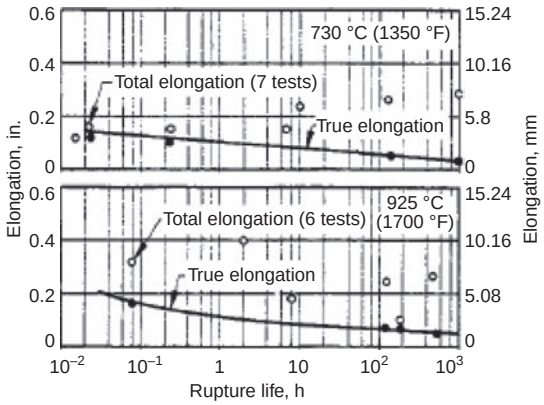

Fig. 8 Relation of elongation and rupture life for Co-Cr-Ni-base alloy S-590 tested at two temperatures at different stresses. Source: Ref 18

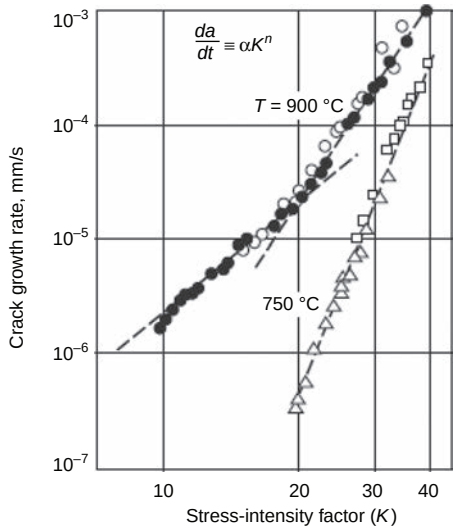

Fig. 10 Power-law dependence of creep crack growth with K in less ductile materials. Source: Ref 19

Stress-Rupture Fracture Characteristics

Stress-rupture fractures are typically characterized by a multiplicity of creep voids at and adjacent to the main fracture, as represented in Fig. 11, which depicts the fractures of a nickel-base turbine blade. The voids are generally easy to identify by light optical examination of cross sections, especially those that include the fracture surface, such as those in Fig. 12, which depicts the microstructure of the failed turbine blade. Figure 13 shows an example of a heater tube that failed by stress rupture and the microvoids that formed near the fracture surface.

Depending on the alloy, temperature, and strain rate, stress-rupture fracture can either be macroscopically brittle or ductile. A macroscale brittle fracture usually is intergranular (IG) and occurs with little elongation or necking. In general, lower creep rates, longer rupture times, and higher temperatures promote IG fractures. Ductile fractures are transgranular (TG) and are typically accompanied by more pronounced elongation and necking. Transgranular creep ruptures, which generally result from high applied stresses (high strain rates), fail by a void-forming process similar to that of microvoid coalescence in dimple rupture. Fracture surfaces of some stress-rupture failures exhibit both TG and IG fracture paths. In such instances, it is usually found that the TG fractures were initiated by prior IG fissures that decreased the cross-sectional area and raised the stress.

Intergranular creep fracture is the more common fracture path for most stress-rupture failures, with low stress and/or high temperature increasing the likelihood of IG fracture. The presence of faceted grain surfaces and associated cracking are common features associated with IG fracture.

However, sometimes IG cracking may not be readily discernible on the surface of a brittle stress-rupture fracture, due to buildup of surface oxides. If oxide buildup is removed, such cracking usually is visible. Intergranular cracking can readily be seen in a polished longitudinal section and can extend beyond the fracture zone.

Intergranular creep fracture depends on the nucleation, growth, and subsequent linking of voids on grain boundaries to form two types of cavities: wedge-type (w-type) cavities or isolated, rounded-type (r-type) cavities. Wedge-type cavities are usually associated with cracking at grain-boundary triple points and are also referred to as triple-point or grain-corner cracks in the literature. Wedge-type cracks form at triple points due to grain-boundary sliding and can be promoted by decohesion at interfaces between grain-boundary precipitates and the matrix. High stresses and lower temperatures promote wedge-crack formation, and wedge cracking at triple points produces a rough fracture surface with identifiable grain-boundary precipitates.

Under low-stress conditions, IG fractures occur by void formation at the grain boundaries. These cavities form along grain edges rather than at grain corners. Because they appear to be round or spherical on metallographic cross sections, these voids are sometimes referred to as r-type cavities.

Other significant microstructural features also are associated with stress-rupture fracture. When IG cracking occurs, crack paths not only follow grain boundaries at and beneath the fracture surfaces, but also grains appear equiaxed even after considerable plastic deformation and total elongation, implying dynamic recrystallization. In contrast, TG fracture frequently exhibits severely elongated grains in the vicinity of the fracture, that is, no recrystallization. Severely distorted annealing twins and deformation bands in face-centered cubic materials can also be seen. The degree of elongation varies with certain metallurgical factors, notably, prior condition of the metal and its susceptibility to recrystallization or grain-boundary migration under given service or test conditions.

Metallurgical Instabilities

Stress, time, temperature, and environment can serve to change the metallurgical structure during service and thus to change the strength. The microstructure of a creep or stress-rupture specimen after elevated-temperature exposure rarely resembles the initial microstructure, and prolonged exposure under creep conditions can result in microstructural changes, such as void formation, the precipitation of new phases, dissolution or growth of desired phases, grain growth, and so on.

A sharp change of slope in a rupture life curve can occur from metallurgical instabilities, such as TG-IG fracture transition, recrystallization, aging or overaging (phase precipitation or decomposition of carbides, borides, and nitrides), intermetallic-phase

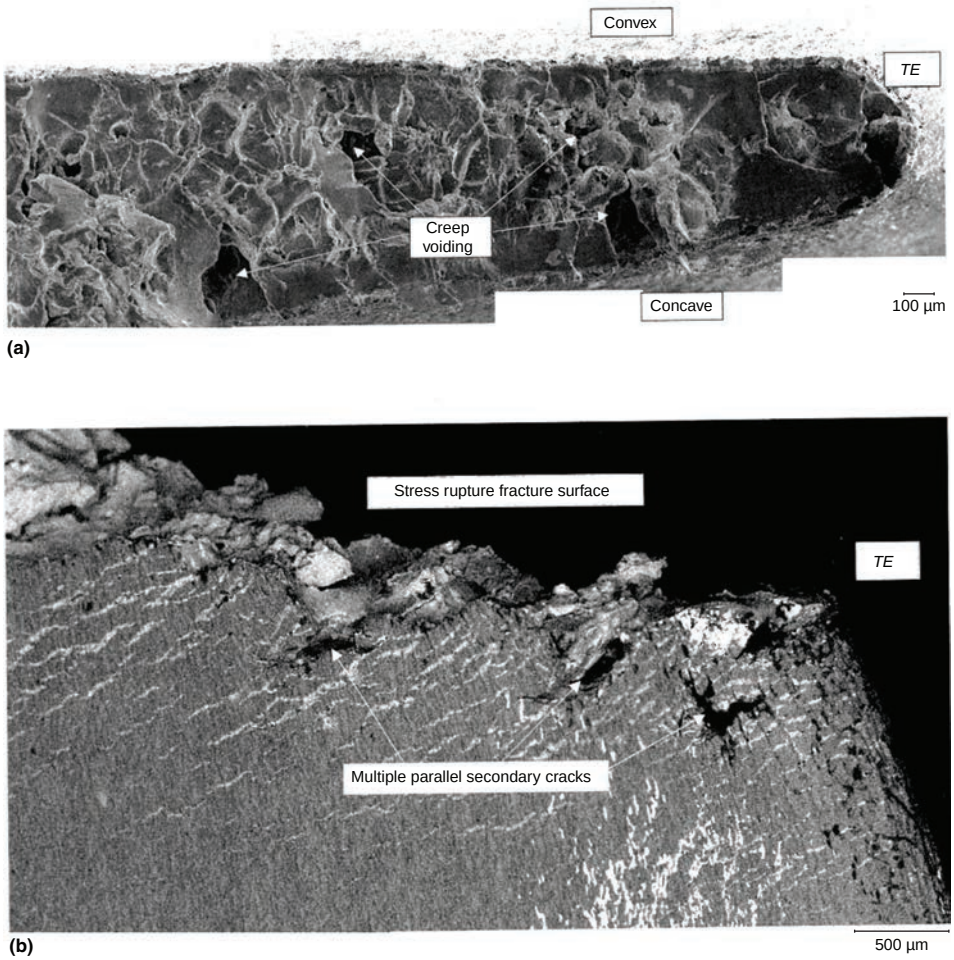

Fig. 11 Fracture surfaces of a nickel-base superalloy turbine blade. (a) Secondary electron image of interdendritic stress-rupture fracture at the trailing edge (TE) of single-crystal turbine blade casting showing creep voids on the fracture surface. (b) Scanning electron microscopy backscatter electron image of stress-rupture cracks and wrinkled aluminide coating on concave trailing-edge side of single-crystal turbine blade casting. Source: Ref 20

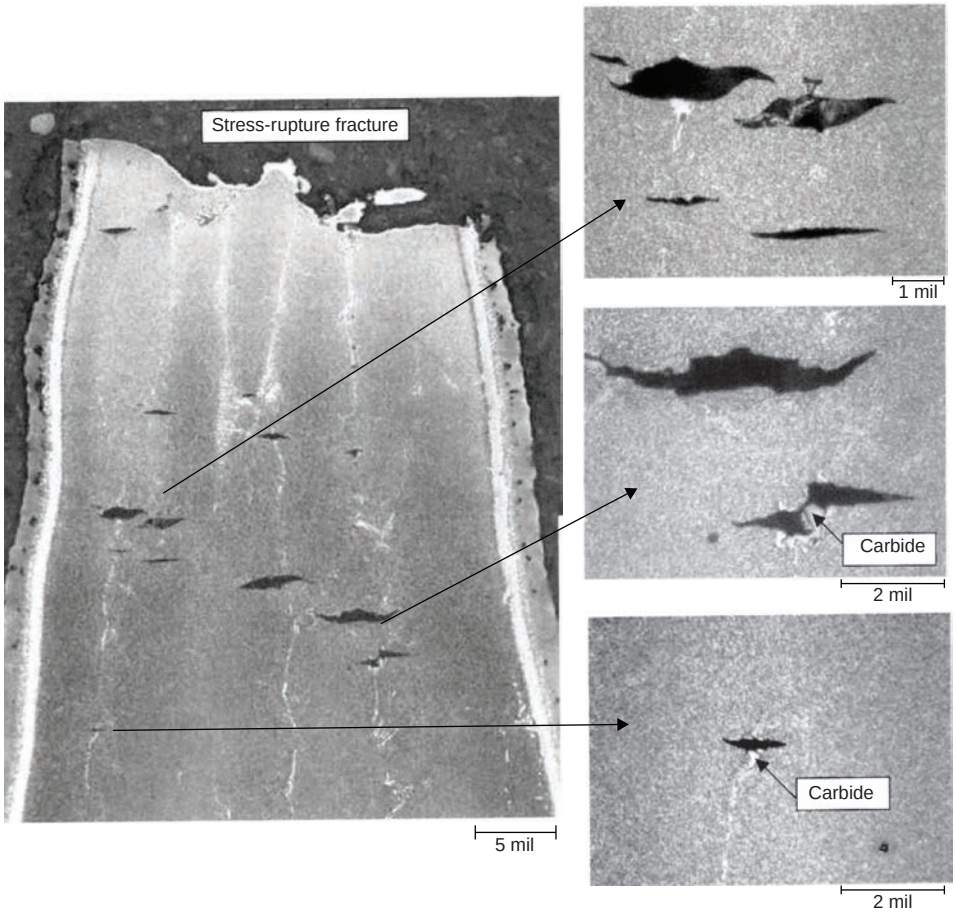

Fig. 12 Creep voids forming near the trailing edge of single-crystal turbine blade casting at ~5% airfoil span. Etchant: 33% glycerol, 33% nitric acid, 33% acetic acid, and 1–3% hydrofluoric acid. Casting contains no grain boundaries. Source: Ref 20

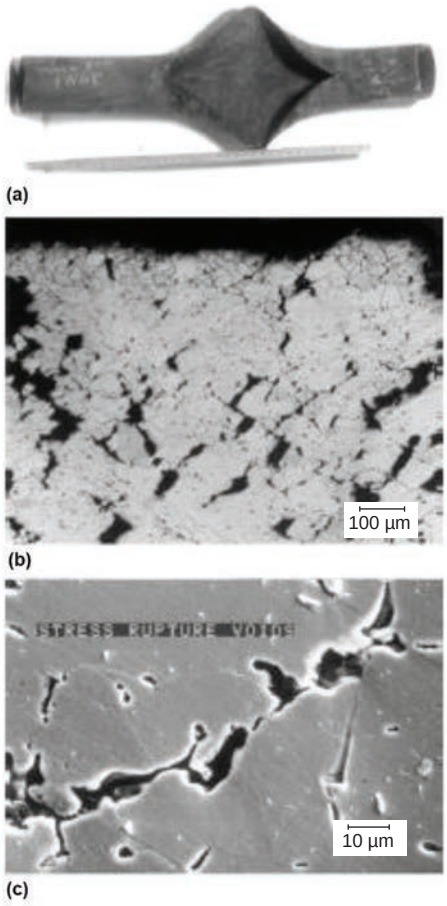

Fig. 13 (a) Heater tube that failed due to stress rupture. (b) and (c) Stress-rupture voids near the fracture. Source: Ref 18

precipitation, delayed transformation to equilibrium phases, order-disorder transition, general oxidation, IG corrosion, stress-corrosion cracking, slag-enhanced corrosion, and contamination by trace elements. Other metallurgical changes (such as spheroidization and graphitization) and corrosion effects can also occur during long-term exposure at elevated temperature. Therefore, mechanical tests after long-term exposure can be useful to determine the effect of these metallurgical changes on short-term or long-term properties.

Transgranular-Intergranular Fracture Transition

The principal metallurgical factor in stress-rupture behavior is the transition from low-temperature TG fracture to high-temperature IG fracture. The transition occurs because the properties of grain-boundary regions differ from those of grains, and the temperature at which the transition occurs is called the equicohesive temperature (ECT), which is analogous to the recrystallization temperature. At low temperatures, grain-boundary regions are stronger than grains, and thus, deformation and fracture are TG. At high temperatures, grain-boundary sliding can occur, making the grain boundaries weaker than grains, and deformation and fracture are largely IG.

The ECT varies with exposure time and stress, and, as such, a specific ECT for a metallic material is only valid under a specific set of conditions. For each combination of stress and rupture life, there is a temperature above which all stress-rupture fractures are IG. For shorter rupture lives and lower stresses, the TG-to-IG transition occurs at higher temperatures. Longer rupture lives and higher stresses occur at lower temperatures. This relationship is illustrated for nickel in Fig. 14. This effect is also illustrated by points *A* and *B* in Fig. 7; points *N*, *O*, and *Y* represent other types of metallurgical instability. Under certain conditions, both TG fracture and IG fracture are found. Consequently, an analysis of rupture life data or component failure is not complete without a thorough metallographic examination to establish the initial failure mechanism.

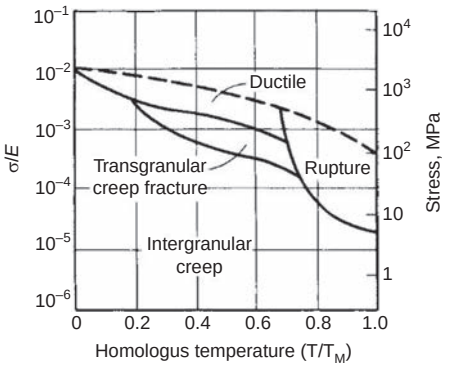

Fig. 14 Fracture mechanism map for nickel. Source: Ref 21

Aging

Age-hardening alloys, which include certain stainless steels, heat-resisting alloys, and aluminum alloys, are characteristically unstable when they are in a state of transition to the

stable (equilibrium) condition. Overaging in alloys can occur when they are exposed to elevated operating temperatures and without being loaded. Under creep conditions, temperature-induced and stress-induced atomic migration usually cause aging to continue, usually resulting in reduced strength. The extent and nature of this change depends on several factors, including the condition of the alloy prior to creep and the temperature, stress, and time of exposure.

Some of the more common high-temperature structural metallic alloys that harden as a result of decomposition of highly supersaturated solid solutions include the Nimonic alloys (Ni-Cr-Al-Ti), austenitic steels that do not contain strong carbide formers, and secondary-hardening ferritic steels. These alloys are widely used for their creep resistance, but they are not immune to reduced rupture life due to overaging.

Intermetallic-Phase Precipitation

In austenitic, high-temperature alloys, topologically close-packed phases (commonly known as tcp), such as sigma, mu, and Laves phases, can form as precipitates at elevated temperatures. The morphology (shape) of these precipitates determines the effect they have on creep strength. For example, needlelike precipitates reduce the toughness and creep strength.

The effects of such phases on rupture life are not well known, but some effects have been studied. For example, the effect of sigma phase (a hard, brittle intermediate phase) on alloy U-700 creep strength at 815 °C (1500 °F) is shown in Fig. 15. Here, a pronounced "break" is shown in the rupture curve starting at approximately 1000 h. Sigma phase was identified in this alloy system and was clearly associated with the failure. However, it was found that sigma did not have a similar effect on certain other nickel-base alloys. Therefore, it must be concluded that sigma phase does not seem to have a universally deleterious effect on stress-rupture behavior. The amount, location, and shape of sigma-phase precipitation determine whether sigma strengthens or weakens an alloy or whether it has no effect. Sigma and other intermetallics can severely reduce ductility and toughness on subsequent cooling to room temperature.

The inconsistency of the effect of sigma-phase formation on creep and stress-rupture properties can arise from the simultaneous presence of other phases, such as carbides. The shape, distribution, and chemistry of carbide particles can influence crack initiation and propagation (thus the resultant stress-rupture ductility and rupture life) in a pronounced manner. It is improbable that sigma phase affects ductility to a significant degree at low strain rates. Consequently, the formation of sigma phase does not necessarily result

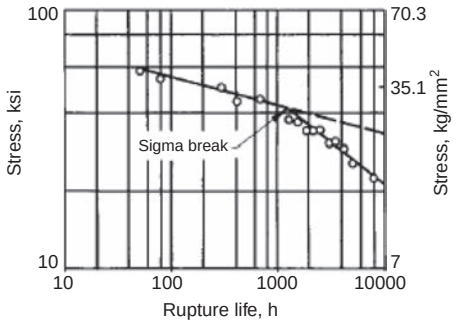

Fig. 15 Logarithmic plot of stress-rupture stress versus rupture life for nickel-base alloy U-700 at 815 °C (1500 °F). The increasing slope of the curve to the right of the sigma break is caused by sigma-phase formation.

in deterioration of creep and stress-rupture properties, unless it is present in relatively large amounts. Therefore, careful metallographic work must be performed on failures to ensure discrimination between sigma-phase-promoted failures and other types of failures in which sigma or other tcp phases are merely present.

Carbide Reactions

Steels and heat-resisting alloys can contain many different types of metallic carbides (M_xC_y). Although temperature and stress affect both carbides within grains and in the grain boundaries, the effects of grain-boundary carbides usually are a more significant factor in altering creep behavior. The presence of carbides is considered necessary for optimal creep and stress-rupture resistance in polycrystalline metals, although subsequent alteration in their shape or breakdown and transition to other carbide forms can be a source of property degradation and resulting failure.

In acicular form, grain-boundary carbides do not appear to necessarily function as brittle notch formers that may directly affect rupture life at elevated temperatures, but they can reduce impact strength. Indirectly, compositional changes from temperature-enhanced diffusion in the vicinity of carbides can alter rupture strength. For example, acicular M_6C carbides generally are not believed to affect the properties of nickel-base high-temperature alloys greatly, unless the alloying elements involved in the carbide reaction alter the matrix composition noticeably. In certain metallic alloys, carbide films formed at grain boundaries can decrease rupture life. Such deleterious films in a Waspaloy forging are shown in the electron micrograph in Fig. 16.

Carbides form in steel when carbon combines with reactive elements, such as titanium, tantalum, hafnium, and niobium. During heat treatment and service, the MC carbide can decompose and generate other carbides, such

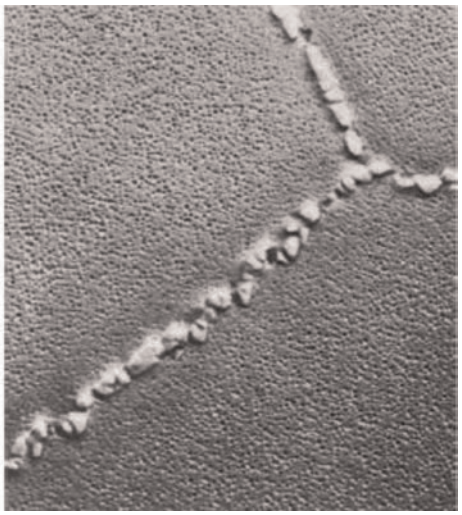

Fig. 16 Grain-boundary carbide films in a Waspaloy forging. The films substantially reduced stress-rupture life. The specimen was electropolished before replication in a solution containing (by volume) 100 parts hydrochloric acid, 50 parts sulfuric acid, and 600 parts methanol. Transmission electron micrograph. Original magnification: 4000×

as $M_{23}C_6$, which tends to form along the grain boundary. Carbide formation and microstructural catalogues are discussed in more detail in the article "Elevated-Temperature Life Assessment for Turbine Components, Piping, and Tubing" in *Failure Analysis and Prevention*, Volume 11 of *ASM Handbook*, 2002. Specific transitions are known for common Fe-Cr-Mo alloys, such as the sequence of carbide formation in Fig. 17 for 2.25Cr-1Mo steel.

Due to the potential microstructural changes that can develop during high-temperature exposure, long-term exposure at elevated temperature can affect short-term and/or long-term properties. For example, the initial microstructure of a creep-resistant chromium-molybdenum steel consists of bainite and ferrite containing Fe_3C carbides, ε-carbides, and fine M_2C carbides. Although many different carbides can be present, the principal carbide phase responsible for strengthening is a fine dispersion of M_2C carbides, where "M" is essentially molybdenum. With increasing aging during high-temperature service, or tempering in the laboratory, a series of transformations of the carbide phases take place that eventually transform M_2C into M_6C and $M_{23}C$ (where the "M" in the latter two metal carbides is mostly chromium). Such an evolution of the carbide structure results in coarsening of the carbides, changes in the matrix composition (that decreases corrosion resistance), and an overall decrease in creep strength. The effect of exposure on the stress-rupture strength of two chromium-molybdenum steels is shown in Fig. 18.

Interaction of Precipitation Processes

The inconsistent behavior of phase precipitation in alloys at elevated temperature is very often caused by the interaction between carbide and tcp phases. Because these constituents do not always react independently but could interact with each other—an interaction that can become extremely complex—a thorough microstructural examination must be made (usually with the aid of an electron microscope) before accurate conclusions can be drawn.

Creep-Rupture Embrittlement

The accumulation of creep damage, in conjunction with metallurgical changes, can cause embrittlement and a reduction in rupture ductility. For example, in low-alloy steels, the accumulation of creep damage has similarities with temper embrittlement but is irreversible. The temperature range of creep embrittlement in low-alloy steels is 425 to 590 °C (800 to 1100 °F) and appears closely related to formation of fine IG precipitates during creep (Ref 23). Impurities such as phosphorus, sulfur, copper, arsenic, antimony, and tin have been shown to reduce rupture ductility in these alloys.

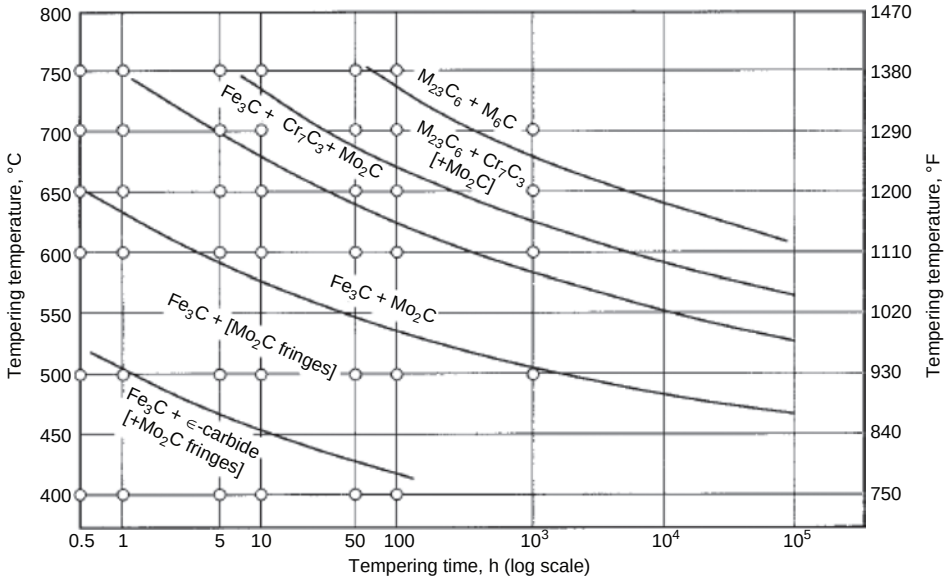

Fig. 17 Isothermal diagram showing the sequence of carbide formation on tempering of normalized 2.25Cr-1Mo steel. Source: Ref 22

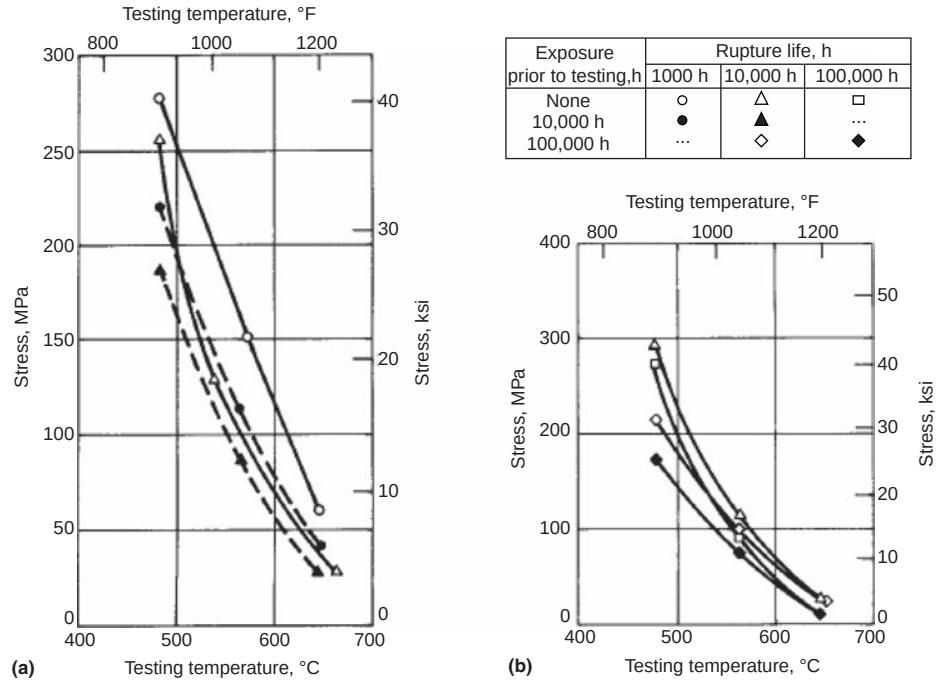

Fig. 18 Effect of elevated-temperature exposure on stress-rupture behavior of (a) normalized and tempered 2Cr-1Mo steel and (b) annealed 9Cr-1Mo steel. Exposure prior to stress-rupture testing was at the indicated test temperatures (without stress) and was 10,000 h long for the 2Cr-1Mo steel and 100,000 h long for the 9Cr-1Mo steel.

Thermal Fatigue and Creep Fatigue

In many high-temperature applications, mechanical conditions and creep are not the only sources of strain. Transient thermal gradients within a component can induce plastic strains, and if these thermal gradients are applied repeatedly, the resulting cyclic strain can induce failure. This process is known as thermal fatigue, where gradual deterioration and eventual cracking of a material occurs from alternating heating and cooling, during which free thermal expansion is partially or fully constrained.

In the past, thermal fatigue traditionally has been treated as synonymous with isothermal low-cycle fatigue (LCF) at the maximum temperature of the thermal cycle. Life-prediction techniques also have evolved from the LCF literature. More recently, advances in finite-element analysis (Ref 24) and testing have made it possible to analyze complex thermal cycles and to conduct thermomechanical fatigue (TMF) tests under controlled conditions. However, isothermal LCF tests and TMF tests should not be considered equivalent, because it has been shown that for the same total strain range, the TMF test can be more damaging under certain conditions than the pure LCF test.

Thermomechanical and combined creep-fatigue loads can result in substantially decreased life at elevated temperatures compared with that anticipated in simple creep loading or isothermal LCF tests. This effect must be considered in failure analysis. When both creep strains and cyclic (i.e., fatigue) strains are present, damage can accumulate from both and can considerably reduce fatigue life and/or creep life. This complex effect is discussed in more detail in the article "Thermomechanical Fatigue: Mechanisms and Practical Life Analysis" in this Volume. Fatigue case studies, in which practical systems are analyzed from a fracture mechanics perspective, are presented in Ref 25. The following is a brief description of thermal-fatigue cracks, as distinguished from creep-rupture cracks.

Thermal-Fatigue Fractures

Thermal-fatigue cracks usually initiate at the surface and then propagate transgranularly inward, perpendicular to the surface and to the plane of maximum normal stress. They

can occur singly or in multiples but often occur in multiples. Because the crack initiates externally, the amount of corrosion or oxidation along the surfaces of a thermal-fatigue crack is inversely proportional to the depth of the crack. Conversely, in stress-rupture cracking, oxidation along the IG crack surface is more uniform.

Excessive creep produces considerable distortion and numerous subsurface cracks, whereas thermal fatigue produces little or no distortion and many surface-initiated cracks. Typically, fracture surfaces of components cracked in stress rupture are irregular and discontinuous, in contrast to the planar, continuous surfaces of thermal-fatigue fractures.

ACKNOWLEDGMENT

This article was revised from "Creep and Stress Rupture Failures," *Failure Analysis and Prevention*, Volume 11, *ASM Handbook*, ASM International, 2002, p 728–737, with additional content from *Fatigue and Fracture*, Volume 19, *ASM Handbook*, ASM International, 1996, and "Elevated-Temperature Failures," Lesson 7, Principles of Failure Analysis, Materials Engineering Institute, ASM International.

REFERENCES

1. F.R.S. Trouton and A.O. Rankine, On the Stretching and Torsion of a Lead Wire Beyond the Elastic Limit, *Philos. Mag. J. Sci.,* Vol 8 (No. 46), 1904, p 538–556
2. P. Phillips, The Slow Stretch of India Rubber, Glass, and Metal Wires When Subjected to a Constant Pull, *Proc. Phys. Soc. London,* Vol 19, 1905
3. E.N. da C. Andrade, On the Viscous Flow in Metals, and Allied Phenomena, *Proc. R. Soc. A,* Vol 84, 1910, p 1–12
4. M. Ezrin, *Plastics Failure Guide: Cause and Prevention,* Hanser Publishers, 1996
5. J. Scheirs, *Compositional and Failure Analysis of Polymers: A Practical Approach,* Wiley, 2000
6. R.W. Hertzberg, *Deformation and Fracture Mechanics of Engineering Materials,* Wiley, 1989
7. K.R. Williams and B. Wilshire, Effects of Microstructural Instability on the Creep and Fracture Behavior of Ferritic Steels, *Mater. Sci. Eng.,* Vol 28, 1977, p 289–296
8. M. Wild, Analyse des Zeitstandverhaltens warmfester ferritischer Stahle bei Temperaturen von 450 bis 600 C, *Arch. Eisenhüttenwes.,* Vol 34, 1963, p 935–950
9. R. Widmer and N.J. Grant, The Role of Atmosphere in the Creep-Rupture Behavior of 80Ni-20Cr Alloys, *J. Basic Eng.* (*Trans. ASME D*), Vol 82 (No. 4), 1960, p 882–886
10. P. Shahinian and M.R. Achter, Creep-Rupture of Nickel of Two Purities in Controlled Environments, *Proc. Joint International Conference on Creep,* Institution of Mechanical Engineers, London, 1963, p 7-49 to 7-57
11. M.V. Nathal and L.J. Ebert, Gamma Prime Shape Changes during Creep of a Nickel-Base Superalloy, *Scr. Metall.,* Vol 17, 1983, p 1151–1154
12. T.H. Courtney, Fundamental Structure-Property Relationships in Engineering Materials, *Materials Selection and Design,* Vol 20, *ASM Handbook,* ASM International, 1997, p 354
13. G. Sposito, C. Ward, P. Cawley, P. Nagy, and C. Scruby, A Review of Non-Destructive Techniques for the Detection of Creep Damage in Power Plant Steels, *NDT & E Int.,* Vol 43 (No. 7), 2010, p 555–567, doi:10.1016/j.ndteint.2010.05.012
14. B. Neubauer and U. Wedel, Rest-of-Life Estimation of Creeping Components by Means of Replicas, *Advances in Life Prediction Methods,* American Society of Mechanical Engineers, 1983, p 307–314
15. J.M. Brear et al., *Possibilitic and Probabilistic Assessment of Creep Damage,* ICM 6, Pergamon, 1991
16. H. Voorhees and M. Prager, Assessment and Use of Creep-Rupture Properties, *Mechanical Testing and Evaluation,* Vol 8, *ASM Handbook,* ASM International, 2000, p 383–397
17. "Fitness-for-Service," API 579/ASME FFS-1, *American Petroleum Institute*, American Society of Mechanical Engineers, June 2016
18. D.J. Benac, "*Elevated-Temperature Failures*," Lesson 7, Principles of Failure Analysis, Materials Engineering Institute, ASM International
19. H. Nelson, "Fractography in the Failure Analysis of Engineering Structures," *presented at ASM International Annual Meeting*, 1997
20. W. Pridemore, Stress-Rupture Characterization in Nickel-Based Superalloy Gas Turbine Engine Components, *J. Fail. Anal. Preven.,* Vol 8, June 2008, p 281–288
21. G.E. Dieter, Evaluation of Workability for Bulk Forming Processes, *Metalworking: Bulk Forming,* Vol 14A, *ASM Handbook*, ASM International, 2005
22. R.G. Baker and J. Nutting, *J. Iron Steel Inst.,* Vol 192, 1959, p 257–268
23. J.J. Hickey and J.H. Bulloch, *Int. J. Pressure Vessels Piping,* Vol 49, 1992, p 339–386
24. M. Metzger and T. Seifert, A Mechanism-Based Model of LCF/HCF and TMF/HCF Life Prediction: Multiaxial Formulation, Finite-Element Implementation and Application to Cast Iron, *Tech. Mech.,* Vol 32, 2012, p 435–445
25. M.H. Aliabadi, Ed., *Thermomechanical Fatigue and Fracture,* WIT Press, 2002